Endocytosis of MHC molecules by distinct membrane rafts

Ruth Knorr, Claudia Karacsonyi and Robert Lindner*

Department of Cell Biology, Hannover Medical School, Carl-Neuberg-Str. 1, 30625 Hannover, Germany

*Author for correspondence (e-mail: lindner.robert@mh-hannover.de)

Summary

In B-lymphocytes, endocytosis of MHC I and MHC II molecules is important for the cross-priming and presentation of labile antigens, respectively. Here, we report that MHC I and MHC II were internalized by separate endocytic carriers that lacked transferrin receptor. Cholera toxin B was co-internalized with MHC II, but not with MHC I, suggesting that the CLIC/GEEC pathway is involved in the uptake of MHC II. Endocytosis of MHC I and MHC II was inhibited by filipin, but only MHC II showed a strong preference for a membrane raft environment in a co-clustering analysis with G_M1. By using a novel method for the extraction of detergent-resistant membranes (DRMs), we observed that MHC I and MHC II associate with two distinct types of DRMs. These differ in density, protein content, lipid composition, and ultrastructure. The results of cell surface biotinylation and subsequent DRM isolation show that precursors for both DRMs coexist in the plasma membrane. Moreover, clustering of MHC proteins at the cell surface resulted in shifts of the respective DRMs, revealing proximity-induced changes in the membrane environment. Our results suggest that the preference of MHC I and MHC II for distinct membrane rafts directs them to different cellular entry points.

Supplementary material available online at
http://jcs.biologists.org/cgi/content/full/122/10/1584/DC1

Key words: Endocytosis, CLIC/GEEC pathway, Major histocompatibility complex, Antigen presentation, Membrane rafts, Detergent-resistant membranes

Introduction

MHC proteins play a pivotal role in the induction and maintenance of adaptive immune responses. MHC I presents peptides to cytotoxic T-lymphocytes, whereas MHC II displays peptides or larger antigen fragments to T-lymphocytes with helper or regulator function (Jensen, 2007). Peptides loaded on MHC I are mainly derived from endogenous antigens. Exogenous antigens can also serve as the peptide source in a process called cross-presentation. This provides an essential priming or tolerizing signal to cytotoxic T-cells (Rock and Shen, 2005). One of the peptide-loading pathways in cross-presentation depends on the endocytosis of surface MHC I and subsequent peptide exchange in endocytic compartments (Di Pucchio et al., 2008; Gromme et al., 1999; Kleijmeer et al., 2001; Liu et al., 1995; Schirmbeck et al., 1995; Tiwari et al., 2007). The peptide cargo of MHC II mostly derives from antigens that have access to late endocytic MHC II loading compartments (Jensen, 2007; Watts, 2004). However, some protease-sensitive determinants associate with MHC II earlier in the endocytic pathway, thereby avoiding destruction by lysosomal cathepsins. This alternative loading pathway relies on the endocytosis of mature MHC II from the cell surface and does not require the cofactors invariant chain and H2-M/HLA-DM (Lindner and Unanue, 1996; Pinet et al., 1994; Pinet et al., 1995; Sinnathamby and Eisenlohr, 2003; Zhong et al., 1997).

No consensus has been reached about the pathways of MHC internalization. MHC I has been localized to clathrin-coated pits (Kleijmeer et al., 2001; Machy et al., 1987) and has been shown to be internalized by clathrin after virus-induced ubiquitinylation (Duncan et al., 2006). However, the single tyrosine-based motif of MHC I used for recognition by clathrin adaptors is dispensable for endocytosis (Vega and Strominger, 1989) and cellular ubiquitin ligases that are capable of modifying MHC I do not localize to the plasma membrane (Bartee et al., 2004). A clathrin- and dynamin-independent internalization route for MHC I that involved cholesterol and the small GTPase Arf6 was discovered in fibroblasts (Naslavsky et al., 2003; Naslavsky et al., 2004). For B-lymphocytes, a common entry pathway of MHC I and MHC II was proposed (Chiu et al., 1999). The cytosolic tail of MHC II β-chain contains a double-leucine motif that lacks the negatively charged groups that are essential for interaction with clathrin adaptors (Bonifacino and Traub, 2003), and its mutation barely affects MHC II endocytosis (Zhong et al., 1997). Ubiquitin ligases of the MARCH family trigger clathrin-mediated endocytosis of MHC II in immature dendritic cells (Shin et al., 2006; van Niel et al., 2006), but not in B-lymphocytes (Matsuki et al., 2007). Therefore, mature MHC proteins are likely to be endocytosed via clathrin-independent routes in B-lymphocytes. Because lymphocytes lack caveolae (Fra et al., 1995), other endocytosis pathways that are dependent on membrane rafts (Mayor and Pagano, 2007) are likely candidates.

Membrane rafts are defined as small, heterogeneous, dynamic, sterol- and sphingolipid-enriched domains that function in the compartmentalization of cellular processes (Pike, 2006). They form larger, long-lived structures upon clustering of their components (Kusumi et al., 2004). A similar induction of large structures (≤1 μm) enriched in membrane raft components is observed after the extraction of membranes with non-ionic detergents at 4°C (Brown and Rose, 1992; Röper et al., 2000) and also at 37°C (Babiychuk and Draeger, 2006; Braccia et al., 2003; Chen et al., 2009; Drevot et al., 2002). It is unclear, however, to what extent such detergent-resistant membranes (DRMs) resemble membrane rafts (Lichtenberg et al., 2005). Membrane rafts depend on cholesterol, a trait that is, however, shared by other cellular processes (Hancock, 2006; Munro, 2003). Nevertheless, there are quantitative differences in cholesterol dependence, as exemplified by the much stronger

inhibition of membrane raft-dependent endocytosis compared with clathrin-mediated internalization by the cholesterol-sequestering drug filipin (Naslavsky et al., 2004; Orlandi and Fishman, 1998). Another feature of membrane rafts is their heterogeneity (Pike, 2004). The standard detergent-based approaches to isolate DRMs have not provided convincing evidence for such a heterogeneity, a failure that fostered the notion that detergent extraction does not yield true membrane rafts (Schuck et al., 2003; Wilson et al., 2004). However, with selective procedures, DRMs have been isolated that reflect some membrane raft heterogeneity (Brügger et al., 2004; Drevot et al., 2002; Madore et al., 1999).

MHC proteins appear to associate with membrane rafts: MHC II has been described as a DRM component and has been observed to co-distribute with the raft marker G_M1 upon antibody-mediated clustering or immunological synapse formation (Rodgers and Smith, 2005). There is biophysical evidence for membrane raft association of MHC I (Bodnar et al., 2003; Matko et al., 1994); however, neither DRM association nor co-patching with G_M1 have been detected (Goebel et al., 2002; Karacsonyi et al., 2004; Naslavsky et al., 2004), except for one report on indirect raft association via ICAM1 (Lebedeva et al., 2004). Although these data suggest that MHC I and MHC II differ in their membrane raft association, a colocalization of MHC I and MHC II in 'supermolecular receptor clusters' has also been reported (Jenei et al., 1997; Vamosi et al., 2004). To clarify this issue, we investigated whether the endocytosis of mature MHC molecules might involve distinct membrane rafts in B-lymphocytes. For this purpose, the endocytic pathways of MHC molecules, their co-clustering with raft markers and their DRM association were investigated. Distinct DRMs were separated by a novel, more rigorous procedure that yielded stable products instead of unstable kinetic intermediates. We also examined whether antibody-mediated clustering leads to a reorganization of DRMs. Such an induced reorganization might mimic early events in MHC endocytosis.

Results

Endocytosis of MHC proteins
MHC proteins enter common endosomal compartments in B-lymphocytes (Chiu et al., 1999), but endosomes serve as a convergence point for various internalization pathways (Mayor and Pagano, 2007). We therefore investigated whether the initial steps of MHC I and MHC II internalization were distinct in mouse B-lymphocytes. For this purpose, the endocytosis of surface-bound anti-MHC antibodies was monitored over a period of 20 minutes in M12.C3.F6 cells. The subcellular distribution of these primary antibodies was revealed with cross-adsorbed secondary reagents and analyzed by confocal laser scanning microscopy. Control incubations with unmatched reagents were used to verify the absence of background signals under our microscope settings. The endocytosis of invariant chain-bound MHC II relative to mature MHC II was negligible, as detailed below. Internalized MHC molecules were detected in distinct peripheral endocytic carriers after 5 minutes (Fig. 1, upper row). These carriers often showed elongated profiles resembling tubules, a feature particularly evident for internalized MHC II molecules upon chemical fixation at 37°C immediately after endocytosis (supplementary material Fig. S1, arrows). Internalized MHC I and MHC II gradually accumulated in common perinuclear endosomes over a 20-minute period (middle rows).

This convergence is also evident from a statistical analysis of confocal sections. Plotting the percentage of internalized vesicles
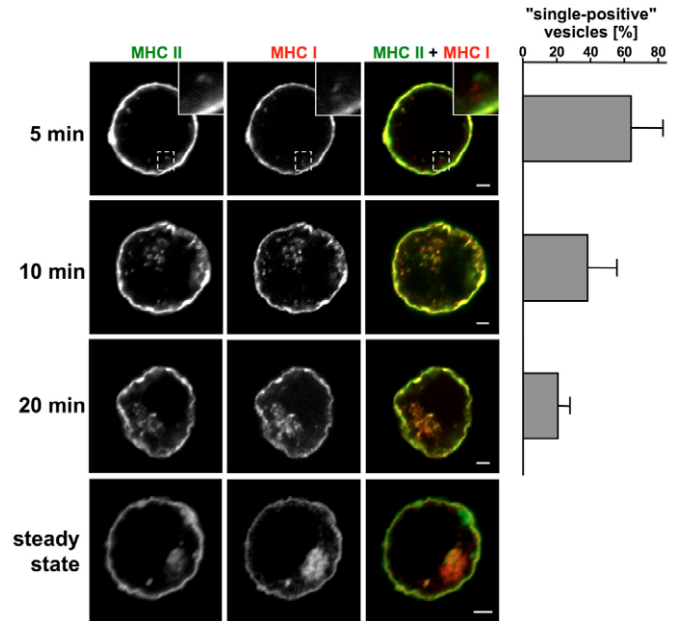

Fig. 1. Internalization of MHC I and MHC II by distinct endocytic carriers in M12.C3F6 cells. Monoclonal antibodies (MAbs) bound to MHC I (R1-9.6) and MHC II (40F) at the cell surface were internalized at 37°C for the indicated times and detected by cross-adsorbed secondary antibodies after fixation and permeabilization. Representative equatorial sections from confocal stacks were selected (rows 1-3). Note that most internalized MHC I and MHC II localized to distinct peripheral structures after 5 minutes, but merged in perinuclear endosomes at 10-20 minutes. (Bottom row) Steady state distribution of MHC proteins in fixed M12.C3.F6 cells. Scale bars: 2 μm. (Left) The staining pattern of endocytic vesicles from 20 equatorial sections per condition was recorded and the percentage of single-positive endocytic vesicles plotted against the endocytosis time. Error bars denote s.d.

containing either MHC I or MHC II against endocytosis time revealed a drop from 64% to 20% of 'single-positive' endocytic vesicles within 20 minutes (Fig. 1, right side). We also observed that about 75% of peripheral endocytic vesicles were 'single-positive', whereas less than 20% of vesicles with a perinuclear location fell into this group. This suggests that distinct peripheral endocytic vesicles fuse either with each other during transit or with common perinuclear compartments upon arrival. Consistent with this interpretation, we detected a substantial overlap in the subcellular distribution of both proteins at steady state (Fig. 1, bottom row). The common perinuclear endosomes reached by MHC proteins after 10-20 minutes of endocytosis contained transferrin receptor (TfnR) (supplementary material Fig. S1). By contrast, the peripheral early endocytic carriers of MHC proteins (5 minutes of endocytosis) were devoid of TfnR (supplementary material Fig. S1). This suggests that MHC proteins use internalization routes that are distinct from that of TfnR.

To further characterize the endocytosis pathways of MHC molecules, we investigated whether they co-internalize with cholera toxin B (CTB). CTB is a ligand for G_M1 and is endocytosed on two pathways, one of which is dependent on clathrin whereas the other does not involve this molecule (Kirkham et al., 2005; Lundmark et al., 2008; Torgersen et al., 2001). As shown in Fig. 2, less than 10% of MHC II-containing early endocytic carriers (5 minutes) were devoid of CTB (i.e. ~90% of internalized MHC II colocalized with CTB). This high degree of colocalization did
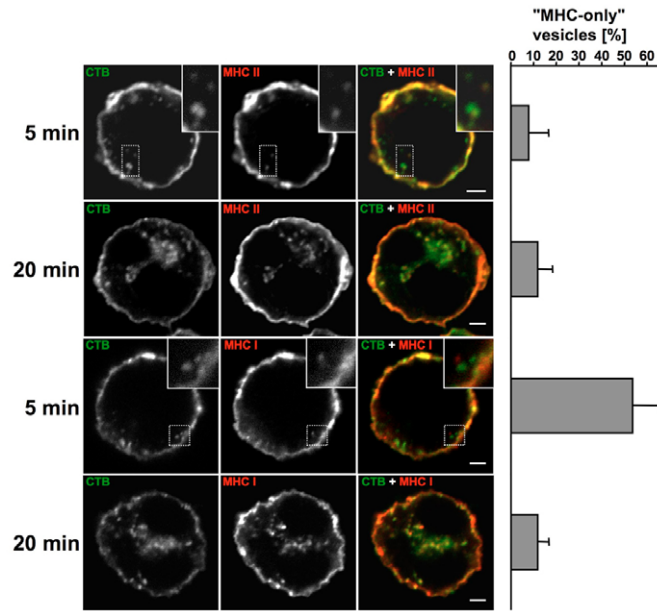
Fig. 2. Co-internalization of MHC molecules with cholera toxin B (CTB). M12.C3F6 cells were labeled with CTB-FITC and either mAb 40F (rows 1-2) or mAb R1-9.6 (rows 3-4) on ice, then warmed to 37°C for 5 or 20 minutes, and stained with secondary reagents after fixation and permeabilization. Rows 1-4 show representative equatorial sections from confocal stacks. (Left) The percentage of MHC-containing vesicles that stained only for MHC and not for CTB-FITC ('MHC-only') is plotted. Per condition 20 equatorial sections were analyzed, error bars denote s.d. Note that most MHC II-positive endocytic vesicles contained CTB at 5 and 20 minutes of endocytosis, whereas MHC I significantly colocalized with CTB only at 20 minutes of endocytosis, and not at 5 minutes (~60% 'MHC I-only' vesicles). Also note the presence of many CTB-containing vesicles devoid of MHC II in the top row. Scale bars: 2 μm.

not significantly change upon transport to perinuclear endosomes (20 minutes). When CTB-positive early endocytic carriers were analyzed, it was evident that only about 50% of CTB-positive structures contained internalized MHC II at 5 minutes (Fig. 2; data not shown), suggesting that a part of the CTB used an endocytosis pathway not related to the uptake of MHC II. By contrast, MHC I appeared largely in vesicles that were devoid of CTB after 5 minutes of endocytosis (~60% of endocytosed MHC I), but reached an MHC II-like level of colocalization with CTB at 20 minutes. At very early

endocytosis times (2.5 minutes), internalized MHC I was completely separated from CTB; however, only a few vesicles were detected per cell (data not shown). Our results suggest that MHC II shares its endocytosis pathway with CTB, whereas MHC I is endocytosed on a different route that subsequently merges with the CTB pathway. We also confirmed the difference in early endocytic carriers of MHC proteins by a biochemical approach. For this purpose, M12.C3.F6 cells were surface-biotinylated with a cleavable biotin derivative, allowed to endocytose for 5 minutes, and stripped of surface biotin (Lindner, 2002). Postnuclear membranes of these cells were fractionated by density gradient electrophoresis (DGE), a method that is capable of separating plasma membrane, biosynthetic membranes and endocytic organelles (Lindner, 2001). Biotinylated MHC I and MHC II molecules were detected in broadly overlapping zones, but at slightly different peak positions, suggesting that the early endocytic carriers of MHC proteins are not identical (supplementary material Fig. S2).

To further characterize the endocytosis of MHC molecules, its kinetics and its sensitivity to filipin was compared with that of TfnR, a well-known cargo of clathrin-coated vesicles. Filipin is thought to form large complexes with cholesterol in the plasma membrane and to prevent the formation of cholesterol-dependent membrane rafts (Bolard, 1986; Orlandi and Fishman, 1998). M12.C3.F6 cells were pre-incubated with or without 15 μM filipin before being surface labeled with a cleavable biotin derivative. The cells were then allowed to endocytose in the presence or absence of filipin. After stripping the surface biotin, endocytosed molecules were detected by their biotin label. As shown in Fig. 3, only few percent of each type of surface MHC molecule was internalized within 8 minutes. Quantitative data were obtained by a comparison of serial dilutions of total surface biotinylated MHC proteins with internalized ones (supplementary material Fig. S3). Invariant chain-driven endocytosis of MHC II accounted for <1% of the endocytosis of mature, invariant chain-free MHC II in M12.C3.F6 cells (supplementary material Fig. S4). Thus, >99% of the endocytosis of MHC II (as determined in Figs 1-3 and supplementary material Figs S1-S2) is driven by mature MHC II. In contrast to the slow internalization of MHC proteins, clathrin-mediated endocytosis of surface TfnR was already complete at 8 minutes (Fig. 3, lower panel). Filipin inhibited the internalization of MHC I and MHC II by >80%, but reduced the endocytosis of TfnR by only 20% at 8 minutes. Thus, the endocytosis of MHC
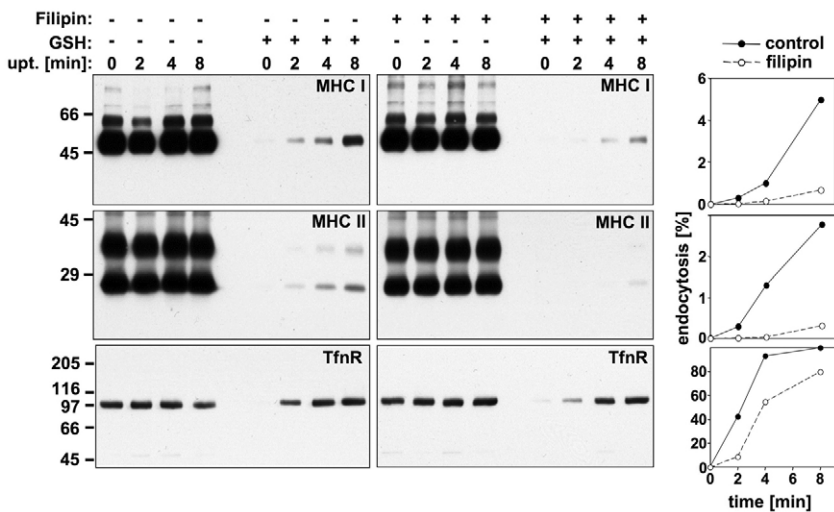

Fig. 3. Cholesterol-dependent endocytosis of MHC proteins. M12.C3.F6 cells were pre-treated or not with 15 μM filipin III before surface biotinylation and internalization in the presence or absence of filipin. Surface biotin was removed by GSH (right) or not (left) and MHC I and MHC II were sequentially immunoprecipitated and probed for biotin (top and middle panel). The remaining biotinylated proteins were retrieved and probed for TfnR (lower panel). MHC proteins were quantified as described in Fig. S3 (see supplementary material), TfnR was quantified by densitometry. Internalization was expressed relative to the mean of samples not stripped by GSH. Shown are results of one experiment out of two with similar results. Note that internalization of MHC proteins was slow and sensitive to filipin, whereas endocytosis of TfnR was fast and almost unaffected by filipin.
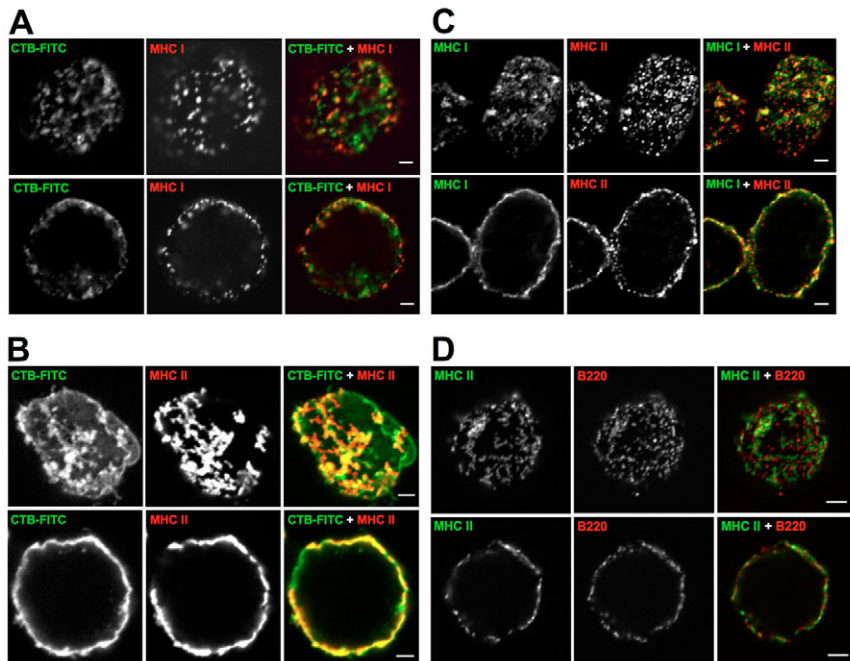
Fig. 4. Analysis of the membrane environment of patched MHC proteins in M12.C3.F6 cells. Clusters of MHC I (A) or MHC II (B) on M12.C3.F6 cells were induced with mAbs R1-9.6 (A) or 40F (B) and appropriate secondary reagents. G_M1 was patched by CTB-FITC. Clusters of MHC II and MHC I (C) or B220 (D) were induced with mAb 40F and mAbs R1-9.6 (C) or RA3-6B2 (D), and cross-adsorbed secondary reagents. Note the extensive co-patching of MHC II and G_M1 (B), the low co-patching of MHC I and G_M1(A), or MHC I and MHC II (C), and its absence from the MHC II-B220 sample (D). Scale bars: 2 μm.

proteins differs in respect to kinetics and filipin sensitivity from that of a typical cargo protein of clathrin-coated pits. MHC proteins therefore appear to be internalized by clathrin-independent pathways (Mayor and Pagano, 2007), which often show a higher dependence on membrane cholesterol (Naslavsky et al., 2004; Orlandi and Fishman, 1998).

Preference of MHC proteins for distinct membrane environments

We next assessed the tendency of MHC proteins to distribute to stabilized membrane rafts. For this purpose, antibodies bound to surface MHC I or MHC II were reacted with cross-adsorbed secondary antibodies. Surface G_M1 was detected with FITC-labeled CTB. Patch formation was induced by brief warming and stopped by chilling and fixation. As shown in Fig. 4A, the pattern of patches for MHC I and G_M1 was different in both tangential and equatorial confocal sections, although a moderate enrichment of G_M1 in some MHC I patches was visible as well. By contrast, patched surface MHC II showed a very good overlap with clustered G_M1 (Fig. 4B). We also investigated to what extent MHC proteins would co-patch, if clustered individually. Control incubations using unmatched reagents did not give any detectable signal under our microscope settings. As shown in Fig. 4C, the overall pattern of staining appeared to be different for MHC I and MHC II in tangential sections. However, in some larger patches colocalization was evident. As a negative control, co-patching of MHC II and B220 (Fig. 4D), a membrane protein excluded from rafts (Anderson et al., 2000), was performed. In this case, no co-patching was detected, suggesting that the occasional colocalized patches observed in Fig. 4C were significant. We conclude that antibody-patched MHC I and MHC II prefer distinct membrane environments on the plasma membrane. This preference is, however, not absolute, as some overlap was evident under our experimental conditions. The membrane environment preferred by clustered MHC II appears to be a raft subtype enriched in G_M1, whereas clustered MHC I partitions to a distinct raft subtype or a non-raft environment.

Distribution of MHC proteins to distinct DRMs

We wondered whether a preference of MHC proteins for distinct membrane environments could be confirmed by the DRM technique. This would require a separation of DRMs with different protein and lipid composition. We tested different extraction protocols for their capability to resolve distinct DRMs. With the standard Triton X-100 (TX-100)-based isolation procedure only a small fraction of MHC I and MHC II floated on gradients devoid of detergent (supplementary material Fig. S5). No difference was evident between the flotation positions of both MHC proteins. Some endoplasmic reticulum (ER)-specific immature invariant chain (Ii_{imm}) floated as well, suggesting that the procedure was not selective for cholesterol- and sphingolipid-rich DRMs absent from the ER (Alfalah et al., 2005). In the continued presence of detergent, no flotation of MHC proteins and little flotation of raft markers were found (supplementary material Fig. S5). This suggests that TX-100 DRMs are sensitive to extended detergent exposure. More rigorous TX-100-based extraction procedures might therefore lead to the disintegration of DRMs rather than to the separation of potential DRM subpopulations. For this reason, we focused on Brij 98 DRMs that are stable upon prolonged detergent exposure (R.L., unpublished data). In the original procedure, cellular membranes were only briefly exposed to detergent (Drevot et al., 2002). Under these conditions, the majority of MHC II and alkaline phosphatase (AP) floated to fractions 8-10 on a linear 10-40% sucrose gradient devoid of detergent (Fig. 5A). Some MHC I was found in an overlapping zone that was poorly resolved from the soluble material. Suspecting incomplete extraction, we increased the on-ice extraction time to ≥14 hours and included 1% Brij 98 in the gradient. With this rigorous procedure, AP and MHC II distributed closer to the top of the gradient (Fig. 5B, light DRMs), whereas MHC I floated closer to the bottom (dense DRMs). Furthermore, DRM-associated MHC I molecules were more focused and better resolved from soluble molecules than were those shown in Fig. 5A. Thus, the rigorous extraction procedure separated DRMs containing MHC I or MHC II. In agreement with earlier results, CD81, a marker for
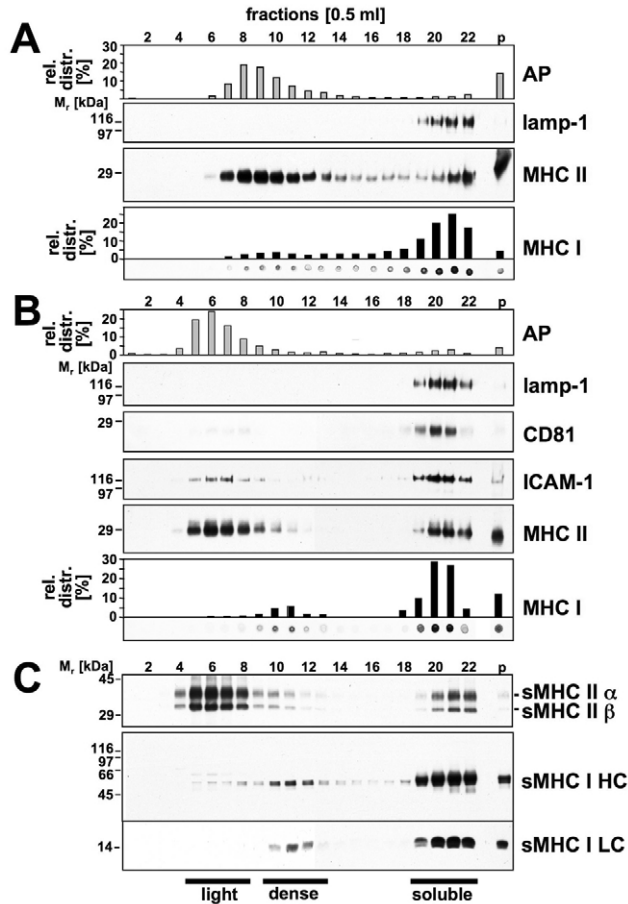
Fig. 5. Separation of MHC I- and MHC II-containing DRMs. (A) Brief Brij 98 extraction following a protocol derived from Drevot et al. (Drevot et al., 2002). (B) Rigorous Brij 98 extraction protocol. (C) Flotation of surface-biotinylated MHC I and MHC II molecules after rigorous Brij 98 extraction. Note that MHC I and MHC II floated to separate fractions in B and C, but not in A. Also note that MHC I- and MHC II-containing DRMs were both derived from the same membrane, the plasma membrane, in C. AP, alkaline phosphatase; sMHC II α,β, cell surface MHC II subunits; sMHC I HC, cell surface MHC I heavy chain; sMHC I LC, cell surface MHC I light chain; rel. distr., relative distribution.

tetraspanin domains at the plasma membrane, was largely solubilized (Karacsonyi et al., 2004). Only residual amounts of this protein were detected in a position close to MHC II-containing DRMs. The maturely glycosylated form of MHC II-associated invariant chain was detected in gradient fractions slightly denser than light DRMs (data not shown), as described earlier (Karacsonyi et al., 2004). Some ICAM1 floated in light DRMs but not in dense ones (Fig. 5B). This was surprising, because ICAM1 has been claimed to interact with MHC I (Lebedeva et al., 2004). However, immunoprecipitation experiments did not provide any evidence for such an association in our cells (Fig. 5C; R.L., unpublished data), suggesting that MHC I floated independently of ICAM1.

The data in Fig. 5B did not provide a clue about whether both types of DRMs were derived from the same or from different cellular membranes. To address this issue, M12.C3.F6 cells were surface-biotinylated with NHSS-LC-biotin and subjected to DRM isolation as in Fig. 5B. After immunoprecipitation, biotinylated MHC I and MHC II were found in the same peak positions and in similar ratios

to their soluble pools (compare Fig. 5B and Fig. 5C). This demonstrates that precursors of dense and light DRMs are present within the same membrane. A key role for light chain-free MHC I heavy chain in the membrane raft association of MHC I has been proposed (Bodnar et al., 2003; Matko et al., 1994). To clarify whether MHC I in dense DRMs contains light chains, the biotinylated MHC I immunoprecipitates were analyzed on 15% acrylamide gels. As shown in Fig. 5C, MHC I light chains were clearly present in dense DRMs. However, our result does not rule out a role of free MHC I heavy chains in MHC I localization to dense DRMs, as the antibody used (R1-9.6) might not recognize free heavy chains, which tend to unfold. Indeed, none of our anti-MHC I antibodies were reactive with denatured MHC I in conventional western blots. For that reason, the distribution of MHC I was assayed by dot blot, a procedure that avoids denaturation.

Polypeptide composition of DRMs containing MHC I and MHC II

To investigate to what extent the two types of DRMs were related, we silver stained the proteins after SDS-PAGE. As shown in Fig. 6A, the polypeptide composition in fractions 5-7 (light DRMs containing AP, G_M1 and MHC II) was clearly different from that in fractions 11-13 (dense DRMs containing MHC I). Only a few polypeptides appeared to occur in both DRMs, ruling out a close relationship. A Coomassie blue-stained gel of concentrated DRMs showed that the overall protein content of dense DRMs was much higher than that of light DRMs (Fig. 6A, bottom right). However, in relation to solubilized material (fractions 19-22, no further concentration), both DRMs (each 33-fold concentrated) contributed only little to the total protein present in postnuclear membranes of M12.C3.F6 (less than 3% of the total postnuclear membrane proteins). To rule out that these results are restricted to a particular cell line, two other commonly used mouse B-cell lines were analyzed (supplementary material Fig. S6). Markers for light DRMs (G_M1) and non-DRM membrane proteins (Lamp1 and CD81) showed a distribution comparable to those of M12.C3.F6. MHC proteins floated similarly in all B-cell lines, although differences were evident in the position and extent of flotation. As judged by silver staining, dense DRMs contained a similar set of proteins in all cell lines; however, light DRMs showed a greater variability. This might be because of the different differentiation stages of the B-lymphoma lines used. Regardless of this issue, MHC proteins were found to co-float with DRMs defined by the two protein peaks. This suggests that MHC I and MHC II are genuine components of dense and light DRMs, respectively, in mouse B-cells.

Ultrastructure, lipid composition and cholesterol dependence
Light and dense DRMs differ in their ultrastructure, as shown by negative staining and ultrathin sectioning (supplementary material Fig. S7). The combination of both techniques demonstrated that light DRMs were composed of flat, round disks of membranes, whereas dense DRMs consisted of composite, curved, open objects. The differences in structure and polypeptide composition suggest that dense and light DRMs may also differ in their lipid constituents. As is evident from Fig. 6A, G_M1 was highly enriched in light DRMs, but was hardly detected in dense DRMs. For further analysis, lipids were extracted from DRMs and postnuclear membranes and analyzed by high-performance thin-layer chromatography (HPTLC). Staining with primulin revealed an enrichment of cholesterol, sphingomyelin (SM)/phosphatidylinositol (PI) and phosphatidylserine in light DRMs relative to the composition in postnuclear membranes (Fig.
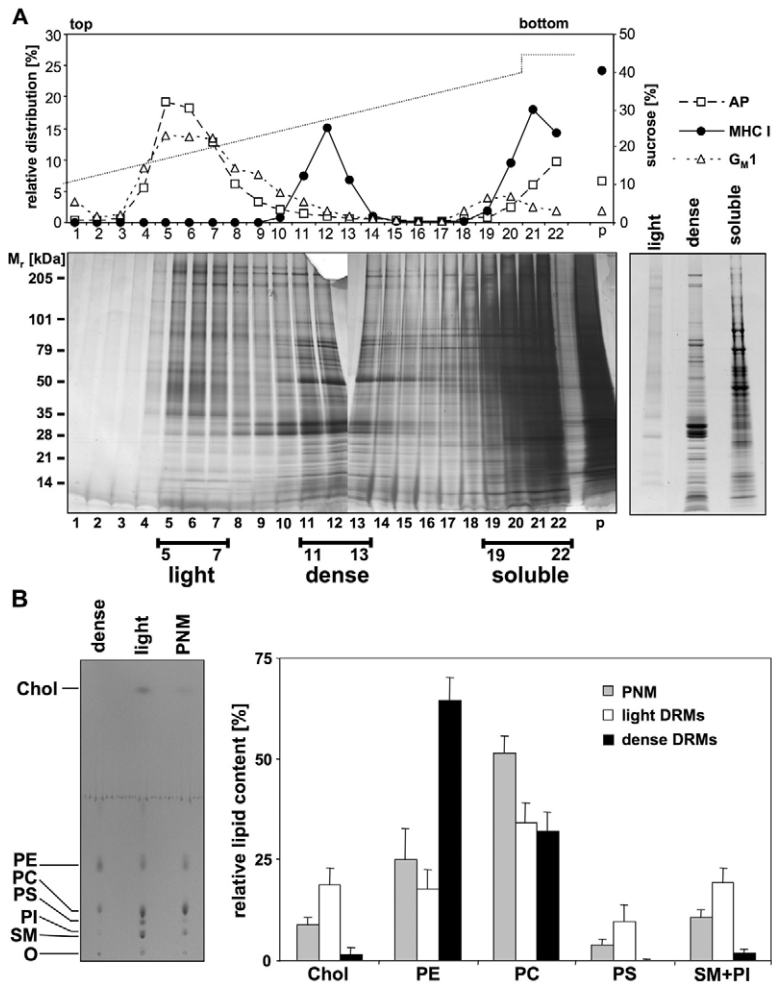
Fig. 6. Polypeptide and lipid composition of dense and light DRMs of M12.C3.F6 cells. (A) DRMs prepared by rigorous Brij 98 extraction at a detergent to protein ratio of 1.25. (Top) Marker profiles. (Bottom left) Protein profile by silver staining. (Bottom right) Coomassie-stained gel of dense and light DRMs, each 33-fold concentrated, and soluble protein (no further concentration). (B) Lipid composition of PNMs and dense and light DRMs. Lipids were extracted from PNMs or from pelleted DRMs, separated by HPTLC, stained with primulin (left), and quantified (right, five independent experiments). The relative lipid content was calculated assuming identical molar primulin adsorption of all lipids. SM and PI were quantified together. Error bars denote s.d. Note the abundance of cholesterol, SM/PI and PS in light DRMs, and of PE in dense DRMs. PC, phosphatidylcholine; PE, phosphatidylethanolamine; PI, phosphatidylinositol; PS, phosphatidylserine; SM, sphingomyelin.

6B). Dense DRMs showed a different lipid composition than light DRMs, with little cholesterol and SM/PI, but with a high prevalence of phosphatidylethanolamine (PE). PE and phosphatidylcholine were the most abundant lipids in dense DRMs, accounting for about 95% of the primulin signal. The low cholesterol content of dense DRMs was surprising in regard of the strong cholesterol dependency of MHC I endocytosis. Therefore, we investigated whether the DRM association of MHC I was dependent on cholesterol. Sequestration of cholesterol by filipin did not destabilize MHC-containing DRMs (R.K. and R.L., unpublished data). We therefore examined the effect of β-methyl-cyclodextrin (MCD), a drug capable of extracting cholesterol from cellular membranes, on the DRM association of MHC I. Cells were treated with 10 mM MCD for 30 minutes at 37°C before DRM isolation. As a positive control for cholesterol depletion, the distribution of MHC II and AP was analyzed. Approximately half of the floating MHC II was solubilized by MCD treatment, whereas the other half shifted to a broad zone in the region of dense DRMs (Fig. 7). This was also observed for AP, suggesting that light DRMs were affected but not completely solubilized under our conditions. By contrast, MCD treatment released 80% of the floating MHC I to soluble fractions (Fig. 7). This suggests that, despite its low level, cholesterol is essential for the stability of MHC I-containing DRMs. This discrepancy might be caused by the heterogeneity of dense DRMs that possibly consist of a minor

cholesterol-dependent, MHC I-positive subpopulation and a major subpopulation that is independent of cholesterol. To clarify this issue, the effect of MCD treatment on the polypeptide composition of dense DRMs was analyzed by silver staining. As shown in Fig. 7 (bottom), polypeptides of light DRMs completely disappeared from their position after MCD treatment, whereas polypeptides of dense DRMs were still present, albeit at a slightly reduced level. Because MHC I levels were diminished by over 80% by this treatment, MHC I-containing DRMs form a minor but distinct subpopulation of dense DRMs. We wondered whether this MHC I-containing subpopulation of dense DRMs also contained sphingolipids, another important lipid component of membrane rafts. There is evidence that distinct membrane rafts in the plasma membrane differ in respect to their G_M1 and G_M3 content (Fujita et al., 2007; Gomez-Mouton et al., 2001). Unfortunately, no G_M3 could be detected in M12.C3.F6 cells (data not shown). However, the sphingolipid G_M2 was present at low amounts in these cells, and it distributed to dense DRMs and to a lesser extent also to light DRMs (Fig. 8A). Clustering revealed its co-distribution with both MHC I and MHC II at the plasma membrane (Fig. 8B). This suggests that G_M2 is a component of both types of membrane environment and that the MHC I-containing subpopulation of dense DRMs may bear some resemblance in structural organization to cholesterol- and sphingolipid-rich light DRMs.
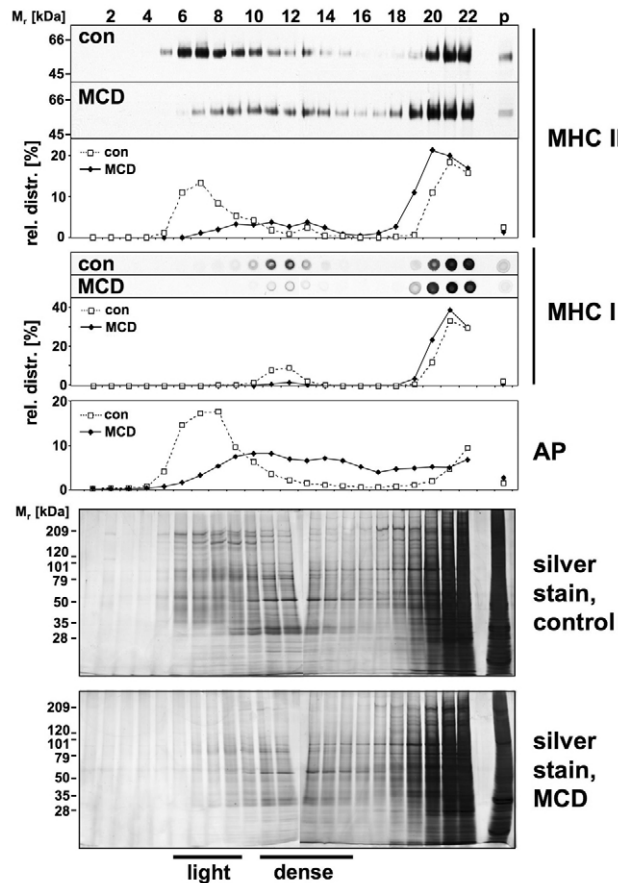
Fig. 7. Sensitivity of dense and light DRMs to cholesterol extraction. M12.C3.F6 cells were extracted with 10 mM MCD or left untreated before PNM preparation and rigorous extraction with Brij 98. In addition to individual proteins, total protein was analyzed by silver staining. Gels from control and MCD-treated samples were stained in one tray for comparability. Note that MHC I, MHC II and light DRM polypeptides were strongly diminished at their DRM position by MCD treatment, whereas polypeptides associated with dense DRMs were only slightly affected. AP, alkaline phosphatase; con, control; MCD, β-methyl-cyclodextrin.

Relationship between DRMs and stabilized membrane rafts

The TX-100 resistance of some membrane raft proteins is enhanced by antibody-mediated clustering/patching (Becart et al., 2003; Harder et al., 1998; Huby et al., 1999), suggesting that this regimen changes the properties of the subsequently extracted DRMs. To investigate this issue for Brij 98 DRMs, we patched MHC molecules on the surface of M12.C3.F6 cells and prepared DRMs by rigorous Brij 98 extraction. Upon patching with MHC I-specific antibodies, more than 90% of MHC I became resistant to Brij 98 extraction and the MHC I-containing DRMs shifted, by about two fractions, closer to light DRMs (supplementary material Fig. S8A). Patching of MHC II also induced high resistance to Brij 98. Antibody-clustered MHC II molecules were shifted by three fractions to the opposite direction (to higher densities, see Fig. S8A), and now overlapped with dense DRMs. Patching of MHC II also co-shifted ~30% of AP and G_M1, which is indicative of the co-recruitment of these markers. By contrast, patching of MHC I had only a small effect on the distribution of AP, G_M1 and mature MHC II. These small shifts were nevertheless specific, as a non-raft protein at the plasma membrane, B220, and ER-localized, immature MHC II α-
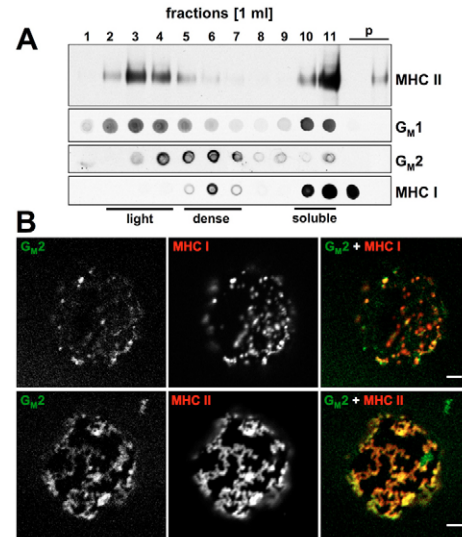

Fig. 8. Distribution of G_M2 to MHC I- and MHC II-containing membrane environments. (A) Localization of G_M2 in dense and light DRMs. Immunoblot analysis of the distribution of MHC I, MHC II, G_M1 and G_M2 after rigorous Brij 98 extraction and flotation. Owing to low G_M2 levels in M12.C3.F6 cells, DRMs were concentrated 20-fold before dot blotting with anti-G_M2. (B) Co-clustering analysis of G_M2 and MHC proteins. G_M2 and MHC I or MHC II were clustered by primary and cross-adsorbed secondary antibodies. Only tangential confocal sections are displayed. Note that both MHC I and MHC II showed co-clustering with patched G_M2. Scale bars: 2 μm.

chain were not affected at all (supplementary material Fig. S8A). Our data thus demonstrate that patching with antibodies at the cell surface specifically changes the properties of the DRMs that contain the targeted molecules. In a search for other putative protein constituents of DRMs, gradient profiles were silver stained and inspected for polypeptides that co-shifted with patched MHC molecules (supplementary material Fig. S8B). We detected a polypeptide of approximately 210 kDa that specifically shifted with MHC I (arrow) and two polypeptides in the 30-50 kDa range that shifted with MHC II (asterisks). Furthermore, our analysis revealed that MHC-containing DRMs were only minor subpopulations, as patching only resulted in density shifts in a few polypeptides.

Discussion

Our results provide several lines of evidence for an involvement of distinct membrane rafts in the endocytosis of mature MHC molecules: (1) MHC proteins preferred distinct membrane environments at the plasma membrane; (2) MHC I and MHC II distributed to chemically distinct types of DRMs; and (3) the endocytosis of MHC molecules showed a high dependence on cholesterol characteristic for membrane raft-mediated endocytosis and it proceeded via two distinct vesicular carriers, both of which were devoid of TfnR.

The membrane environment of MHC proteins

Antibody-mediated clustering has been widely used to obtain information about the membrane environment of molecules. Although this technique does not report on the environment of membrane molecules before patching, it reveals a tendency of closely apposed membrane molecules to assemble a specific environment such as a raft. Co-patching of MHC II and G_M1 has

been reported, but MHC I has not been found to co-cluster with this molecule (Anderson et al., 2000; Goebel et al., 2002; Huby et al., 1999; Karacsonyi et al., 2004). We confirmed these data and also demonstrated that there was only limited co-patching of MHC I and MHC II, suggesting that these proteins prefer distinct membrane environments. Our results are at variance with studies that reported a co-distribution of MHC I with MHC II even in the absence of experimental clustering (Chiu et al., 1999; Jenei et al., 1997; Szollosi et al., 1996; Vamosi et al., 2004). We cannot rule out that patching of MHC proteins releases them from any pre-existing clusters. Evidence for such a reorganization has been obtained for GPI-anchored proteins, which dissociated from highly dynamic nanoclusters and switched internalization pathways upon patching (Sharma et al., 2004). However, we consider pre-existing clusters containing both MHC I and MHC II to be unlikely in our cells, because: (1) two different procedures, detergent extraction and patching, provided evidence for the distinct preferences of MHC molecules; (2) endocytosis of MHC I and MHC II proceeded on different pathways; and (3) there is biophysical evidence that MHC II molecules do not diffuse in higher association states without patching (Umemura et al., 2008; Vrljic et al., 2002).

Distribution of MHC proteins to chemically distinct DRMs

Attempts to separate different types of DRMs supported the notion that chemically distinct DRMs might exist (Brügger et al., 2004; Drevot et al., 2002; Röper et al., 2000). Our work continues on these lines and shows for the first time a direct separation of two chemically distinct DRMs derived from a single subcellular compartment. The distribution of MHC proteins to distinct DRMs correlated with the preference for different membrane environments and with the selection of separate endocytic pathways, implicating the association with distinct membrane rafts as the common cause. However, observations of detergent-induced formation of DRMs on synthetic membranes devoid of rafts (Heerklotz, 2002) and of PIP2 patches in living cells (van Rheenen et al., 2005) place doubt on a close correlation between DRMs and membrane rafts. Consistent with artificial induction, our Brij 98 DRMs are larger than membrane rafts observed in live cells [30-500 nm (see Fig. S7 in the supplementary material), versus 5-30 nm (Prior et al., 2003; Sharma et al., 2004)]. However, the observation of two chemically distinct DRMs suggests that Brij 98 induced homotypic coalescence of DRM precursors, thus avoiding mixing. These DRM precursors might correspond to the dynamic 'nanoclusters' observed in live cells (Sharma et al., 2004) or to lipid shells (Anderson and Jacobson, 2002).

MHC II has been shown by us and many others to be associated with DRMs (Anderson et al., 2000; Becart et al., 2003; Bouillon et al., 2003; Goebel et al., 2002; Hiltbold et al., 2003; Huby et al., 1999; Karacsonyi et al., 2005; Karacsonyi et al., 2004; Meyer zum Bueschenfelde et al., 2004; Setterblad et al., 2004; Setterblad et al., 2003). To our knowledge, this study is the first report showing a direct and cholesterol-dependent DRM association for MHC I, an observation that is consistent with its filipin-sensitive internalization pathway (Fig. 3) (Naslavsky et al., 2004). The cholesterol dependence, the presence of G_M2 in dense DRMs, and its co-patching with MHC I suggest that the MHC I-containing subpopulation of dense DRMs might be organized similarly to cholesterol- and sphingolipid-rich membrane rafts. Some MHC I-related CD1 molecules, which function in the presentation of lipid antigens, have also been shown to be associated with DRMs (Sloma et al., 2008). However, this property appears to be controlled by

invariant chain, a molecule that floated closer to light than to dense DRMs in our gradients (data not shown). We therefore would predict that invariant chain-dependent CD1 molecules are not components of dense DRMs.

Antibody-mediated clustering (patching) is thought to stabilize membrane rafts by inducing their coalescence, which in turn increases the resistance to detergent (Harder et al., 1998). For MHC II, moderate to strong increases in detergent resistance have been reported after patching (Becart et al., 2003; Huby et al., 1999), consistent with our data (supplementary material Fig. S8). We found a similar increase for MHC I, underscoring its affinity for membrane rafts. Furthermore, specific density shifts were observed after patching. These were probably caused by the antibodies and the recruitment of additional membrane components to cell surface patches. Clustering antibodies should increase the density of DRMs, as observed for MHC II. Shifts to lower density might be caused by the recruitment of cytoskeletal proteins (Holowka et al., 2000; Setterblad et al., 2003). The opposite shift of MHC I DRMs, however, can only be explained by a substantial recruitment of low-density membrane components, consistent with an induced reorganization of the DRM. Apart from small amounts of G_M1 and AP, we detected a ~210 kDa polypeptide that specifically shifted with MHC I. The latter polypeptide is the first candidate marker for a stabilized MHC I raft. It is also interesting that the patching of MHC molecules resulted in co-shifts of only a few proteins, suggesting that most dense and light DRMs did not contain MHC proteins. In line with this, MHC I DRMs formed a small, MCD-sensitive subpopulation of dense DRMs (Fig. 7). The presence of multiple types of Brij 98-resistant membranes might reflect the heterogeneity of membrane rafts (Jacobson et al., 2007; Pike, 2004).

Endocytosis of MHCs on separate membrane raft internalization pathways

Our work has revealed a correlation between the internalization of MHC I and MHC II into separate, TfnR-negative endocytic carriers, and their preference for distinct membrane rafts as measured by cell biological and biochemical assays. It suggests that MHC proteins use different entry mechanisms, both of which are strongly cholesterol dependent. Our results are at variance with a study proposing a common endocytic pathway for MHC I and MHC II (Chiu et al., 1999). In this study, however, endocytosis was analyzed only at time points after the separate pathways merged, as revealed in our analysis. Moreover, we observed slow and highly filipin-sensitive endocytosis of MHC proteins that was contrasted by the fast and barely filipin-sensitive endocytosis of TfnR. In line with this, early endocytic carriers for MHC molecules were devoid of TfnR (supplementary material Fig. S1). These results suggest that MHC proteins internalize on clathrin-independent routes in mouse B-cells. An ARF6-regulated recycling pathway has been described for MHC I and for a GPI-anchored protein in human fibroblasts (Naslavsky et al., 2004). It involves tubular, ARF6-positive endosomes transited en route to conventional, RAB5-positive early endosomes. Our data on DRM association, cholesterol-dependent endocytosis and the morphology of early endocytic carriers are consistent with such a pathway. By contrast, the ability of MHC II to co-internalize with a part of CTB (Fig. 2), and to co-recruit G_M1 and a GPI-linked protein after patching (Fig. 4, supplementary material Fig. S8), suggests that MHC II might enter via the so-called CLIC/GEEC pathway. This Cdc42-, ARF1- and GRAF1-regulated route mediates bulk flow endocytosis in fibroblasts and is a major uptake pathway for CTB/G_M1 and for GPI-linked proteins

(Kirkham et al., 2005; Kumari and Mayor, 2008; Lundmark et al., 2008; Sabharanjak et al., 2002). The study of Lundmark et al. also provided evidence for cold-sensitive tubular carriers involved in the uptake via this pathway (Lundmark et al., 2008), consistent with our observations (supplementary material Fig. S1). The ARF6- and the Cdc42/ARF1-regulated pathways are thought to converge on conventional early endosomes (Mayor and Pagano, 2007), again in agreement with our findings. Shortly before this manuscript was submitted a study appeared providing evidence for clathrin- and dynamin-independent endocytosis of MHC II into ARF6$^+$RAB35$^+$EHD1$^+$ endosomes in human antigen-presenting cells (Walseng et al., 2008). Although partially consistent with the data presented here, this study implies a common entry pathway for MHC I and MHC II. Similar to others (Chiu et al., 1999), however, the authors base their conclusions on marker colocalization at endocytosis times (30 minutes) after the merge of the MHC entry pathways (see Fig. 1).

   Why are there two distinct endocytosis pathways for MHC molecules to common endosomes? These pathways might be just a functional consequence of the different membrane raft preferences of MHC molecules. In B-cells, which co-express MHC I and MHC II, such differential preferences might foster the functional separation of immunological synapses formed with CD8$^+$- and CD4$^+$-T-cells, respectively. A distinct membrane raft preference of MHC proteins could also influence their endosomal sorting. MHC II recycles through non-proteolytic, early endosomal compartments without reaching late endocytic organelles (Griffin et al., 1997; Lindner, 2002; Lindner and Unanue, 1996; Pinet et al., 1995). On this recycling route, MHC II is (re)loaded with peptides and proteins by an exchange mechanism (Griffin et al., 1997; Lindner and Unanue, 1996; Pathak and Blum, 2000; Sinnathamby and Eisenlohr, 2003). By contrast, low pH, proteolytic, late endocytic organelles have been proposed as the peptide-loading compartments in MHC I cross-presentation (Gromme et al., 1999; Lizee et al., 2003), but very recent work also invokes early endosomal compartments (Di Pucchio et al., 2008). It will be challenging to elucidate the sorting mechanisms that govern the access to and the egress from loading compartments of these non-classical antigen-presentation pathways.

Materials and Methods
Reagents
Antibodies against CD81 (EAT-1), B220 (RA3-6B2), TfnR (C2) and Lamp1 (1D4B) were from BD Biosciences, those against ICAM1 (KAT-1) were from Fitzgerald and those against G_M2 were from Calbiochem. The anti-MHC I antibody 30-5-7 was a kind gift from Ted Hansen (Washington University, St Louis, MO). Other antibodies (40F, 10.2.16, In-1 and R1-9.6) were produced from cell culture supernatants (Lindner, 2002). The anti-A$^k\alpha$-chain antibody has been described previously (Lindner, 2001). CTB and an anti-CTB antibody were obtained from Quadratech. Secondary antibodies were bought from Dianova, DAKO or Invitrogen. ProLong antifade was obtained from Invitrogen. Neutravidin-HRP, NHSS-LC-biotin, NHSS-SS-biotin and the BCA protein assay were from Pierce. Protein A- and protein G-sepharose and ECL film were bought from Amersham. Western Lightning ECL reagent was from NEN. Sucrose, β-octylglucoside, and DNase I were obtained from Calbiochem. Brij 98, FITC-labeled cholera toxin B-subunit, MCD, poly-L-lysine, glutathion and filipin III were bought from Sigma. Nitrocellulose membrane (BA83) was obtained from Millipore. Glutaraldehyde and osmium tetroxide were purchased from Polysciences. HPTLC 20×20 cm aluminum sheets coated with silica gel 60 were from Merck/VWR. All other chemicals were analytical grade and were obtained from Sigma or Merck/VWR.

Cells
The B-cell line M12.C3.F6 and the hybridoma lines 40F, 10.2.16, In-1 have been described previously (Lindner, 2002). They and the B-cell lines TA3 (Glimcher et al., 1983) and CH27 (Haughton et al., 1986), and the hybridoma R1-9.6 (anti-mouse MHC I) (Koch et al., 1983), were cultured in RPMI 1640 Glutamax I supplemented with 1 mM pyruvate, 100 U/ml penicillin and 100 μg/ml streptomycin, 10 mM HEPES, pH 7.3, 50 μM β-mercaptoethanol (Invitrogen) and 10% fetal calf serum (Biochrom).

Immunofluorescence assay for endocytosis
M12.C3.F6 cells (1×10^6) were incubated with antibodies and/or CTB-FITC at 10 μg/ml in 100 μl endocytosis medium (EM: RPMI 1640 Glutamax I supplemented with 1 mM pyruvate, 100 U/ml penicillin, 100 μg/ml streptomycin, 10 mM HEPES and 0.1% or 1% BSA) for 45 minutes on ice. After washing, the cells were resuspended in 200 μl pre-warmed EM for 2.5-20 minutes at 37°C or kept on ice. Endocytosis was stopped with 1 ml cold HBSS. Cells were fixed with 4% paraformaldehyde in PBS, quenched with 50 mM NH$_4$Cl in PBS, washed and transferred onto poly-L-lysine-coated glass coverslips. Alternatively, cells were fixed immediately after endocytosis by dilution in 1.4 ml pre-warmed 4% paraformaldehyde and a 4-minute incubation at 37°C. Then the cells were quenched and transferred onto coverslips. After permeabilization with 0.05% saponin in PBS and blocking (BB: 1% BSA, 0.05% saponin, 0.02% NaN$_3$ in PBS), the cells were incubated with cross-adsorbed secondary antibodies (5 μg/ml in BB) for 45 minutes at room temperature, washed in PBS, mounted in ProLong antifade medium and inspected on a Zeiss 510 confocal laser scanning microscope. Appropriate photomultiplier settings were obtained with controls stained with mismatched primary and secondary antibodies.

Antibody-mediated clustering of MHC proteins
M12.C3.F6 cells (1×10^6) were incubated with 10 μg/ml primary antibodies (40F, R1-9.6 or anti-G$_M$2) in washing buffer (WB: 1% BSA in HBSS) for 45 minutes on ice. Incubation with secondary antibodies (5 μg/ml in WB) and/or CTB-FITC (1 μg/ml in WB) was for 45 minutes on ice. After several washes, the cells were resuspended in 100 μl cold WB and incubated for 5 minutes at 37°C for patching. The cells were washed again, fixed with 4% paraformaldehyde, quenched with 50 mM NH$_4$Cl in PBS, and transferred onto poly-L-lysine-coated coverslips. Mounting and analysis was carried out as described above.

Surface biotinylation and endocytosis
Surface biotinylation was done as described (Lindner, 2002). For detergent extraction experiments, 5×10^7 M12.C3.F6 cells were biotinylated with non-cleavable NHSS-LC-biotin. For endocytosis experiments, M12.C3.F6 cells (3×10^7 per time point) were surface biotinylated with NHSS-SS-biotin. Endocytosis was started by incubating the cells in pre-warmed EM for 2-8 minutes at 37°C and stopped by adding ice-cold EM. Subsequently, surface biotin was removed by GSH-stripping and the cells were processed for sequential immunoprecipitation as described (Karacsonyi et al., 2004; Lindner, 2002).

Isolation of detergent-resistant membranes
Detergent extractions were performed on post-nuclear membranes (PNMs) prepared as described (Karacsonyi et al., 2004; Lindner, 2002). All extractions were performed at protein concentrations of 4-6 mg/ml and detergent to protein ratios of 1.7 to 2.5 (w/w). To all extracts, DNase I at 100 μg/ml was added. For extraction with TX-100, a published protocol was used with slight modifications (Anderson et al., 2000; Karacsonyi et al., 2005): PNMs were resuspended in 500 μl MES buffer (20 mM MES, 150 mM NaCl, 0.02% NaN$_3$) supplemented with 1% TX-100 and protease inhibitors (5.1 μg/ml leupeptin, 0.1 mM PMSF, 1 μg/ml E-64, 1 μg/ml pepstatin and 5 mM iodoacetamide) and extracted for 1 hour on ice. Then, 500 μl of cold 90% sucrose in MES buffer were added and a linear 10-40% sucrose gradient (in MES buffer and protease inhibitors ±1% TX-100) was poured onto the sample. The gradient was ultracentrifuged at 247,400 × g for 18.5 hours in a Beckman SW41 rotor and fractionated. In the short Brij 98 extraction procedure (Drevot et al., 2002), PNMs were resuspended in 450 μl of MES buffer and protease inhibitors. After warming to 37°C, 50 μl of 10% Brij 98 was added, then samples were incubated for 5 minutes at 37°C, chilled on ice (~1 hour) and mixed with 500 μl of 90% sucrose dissolved in MES buffer. Gradients (devoid of Brij 98) and centrifugation were as described above. In the rigorous Brij 98 extraction procedure (Karacsonyi et al., 2004), PNMs were resuspended in 500 μl of MES buffer supplemented with 1% Brij 98 and protease inhibitors (MB$^+$) and lysed on ice for ~14 hours, followed by 5 minutes at 37°C. The reversed extraction order, with the 37°C step first, yielded similar results. The extract was then mixed with 500 μl of 90% sucrose in MB. Gradients (in MB$^+$) were poured and centrifuged as above.

Density gradient electrophoresis
Density gradient electrophoresis (DGE) was performed as described earlier (Lindner, 2001; Lindner, 2002). Before processing for DGE, the cells (3×10^7) were passed through a biotinylation/endocytosis experiment as detailed above.

Protein methods
SDS-PAGE, immunoblotting and densitometric quantification were performed as described (Karacsonyi et al., 2004). For total protein analysis, standard Coomassie staining or a silver staining procedure (Morrissey, 1981) were used. Sequential immunoprecipitation was performed as described (Karacsonyi et al., 2004; Lindner, 2002).

Perturbation of membrane cholesterol
For sequestration of membrane cholesterol, M12.C3.F6 cells were pre-incubated with 15 μM filipin III in endocytosis medium (EM) at 37°C for 30 minutes. After surface

biotinylation, endocytosis was done in EM at 37°C in the continued presence of filipin III. For extraction of membrane cholesterol, washed M12.C3.F6 cells were incubated in pre-warmed RPMI 1640 containing 10 mM MCD for 30 minutes at 37°C. After one gentle wash with HBSS, post-nuclear membranes were prepared.

Lipid analysis and enzymatic reactions

DRM fractions (derived from 1.8×10^8 cells) were pooled, mixed with 1:3 with cold MES buffer (20 mM MES, 150 mM NaCl, 0.02% NaN$_3$) and spun at $100,000 \times g$ for 2 hours at 4°C. Lipid was extracted from pelleted DRMs or post-nuclear membranes (PMNs, derived from 3×10^7 cells) as described earlier (Karacsonyi et al., 2005). Alkaline phosphatase and β-hexosaminidase were analyzed as described (Karacsonyi et al., 2004; Lindner, 2001).

Electron microscopy

For negative staining, light and dense DRM fractions were adsorbed onto carbon film and contrasted with uranylacetate according to published procedures (Valentine et al., 1968). For ultrathin sectioning, light and dense DRM fractions were diluted 1:3 in MES buffer and centrifuged in a TLA 100.4 rotor (Beckman, $439,800 \times g$, 1 hour, 4°C). Pellets were fixed in 2.5% glutaraldehyde in sodium cacodylate buffer (pH 7.3, 0.1 Osm) at 4°C. The specimens were post-fixed in 1.5% OsO$_4$ and 0.7% K$_3$[Fe(CN)$_6$] for 1 hour at room temperature, dehydrated in ethanol (50, 75, 90, 100% and embedded in epon. Ultrathin sections were cut on an LKB Ultratome III (Bromma, Sweden), stained with uranylacetate and lead citrate, and examined in a Philips EM301 microscope at 80 kV.

References

Alfalah, M., Wetzel, G., Fischer, I., Busche, R., Sterchi, E. E., Zimmer, K. P., Sallmann, H. P. and Naim, H. Y. (2005). A novel type of detergent-resistant membranes may contribute to an early protein sorting event in epithelial cells. *J. Biol. Chem.* **280**, 42636-42643.

Anderson, H. A., Hiltbold, E. M. and Roche, P. A. (2000). Concentration of MHC class II molecules in lipid rafts facilitates antigen presentation. *Nat. Immunol.* **1**, 156-162.

Anderson, R. G. W. and Jacobson, K. (2002). A role for lipid shells in targeting proteins to caveolae, rafts, and other lipid domains. *Science* **296**, 1821-1825.

Babiychuk, E. B. and Draeger, A. (2006). Biochemical characterization of detergent-resistant membranes: a systematic approach. *Biochem. J.* **397**, 407-416.

Bartee, E., Mansouri, M., Hovey Nerenberg, B. T., Gouveia, K. and Fruh, K. (2004). Downregulation of major histocompatibility complex class I by human ubiquitin ligases related to viral immune evasion proteins. *J. Virol.* **78**, 1109-1120.

Becart, S., Setterblad, N., Ostrand-Rosenberg, S., Ono, S. J., Charron, D. and Mooney, N. (2003). Intracytoplasmic domains of MHC class II molecules are essential for lipid-raft-dependent signaling. *J. Cell Sci.* **116**, 2565-2575.

Bodnar, A., Bacso, Z., Jenei, A., Jovin, T. M., Edidin, M., Damjanovich, S. and Matko, J. (2003). Class I HLA oligomerization at the surface of B cells is controlled by exogenous beta(2)-microglobulin: implications in activation of cytotoxic T lymphocytes. *Int. Immunol.* **15**, 331-339.

Bolard, J. (1986). How do the polyene macrolide antibiotics affect the cellular membrane properties? *Biochim. Biophys. Acta* **864**, 257-304.

Bonifacino, J. S. and Traub, L. M. (2003). Signals for sorting of transmembrane proteins to endosomes and lysosomes. *Annu. Rev. Biochem.* **72**, 395-447.

Bouillon, M., El Fakhry, Y., Girouard, J., Khalil, H., Thibodeau, J. and Mourad, W. (2003). Lipid raft-dependent and -independent signaling through HLA-DR molecules. *J. Biol. Chem.* **278**, 7099-7107.

Braccia, A., Villani, M., Immerdal, L., Niels-Christiansen, L. L., Nystrom, B. T., Hansen, G. H. and Danielsen, E. M. (2003). Microvillar membrane microdomains exist at physiological temperature. Role of galectin-4 as lipid raft stabilizer revealed by "superrafts". *J. Biol. Chem.* **278**, 15679-15684.

Brown, D. A. and Rose, J. K. (1992). Sorting of GPI-anchored proteins to glycolipid-enriched membrane subdomains during transport to the apical cell surface. *Cell* **68**, 533-544.

Brügger, B., Graham, C., Leibrecht, I., Mombelli, E., Jen, A., Wieland, F. and Morris, R. (2004). The membrane domains occupied by glycosylphosphatidylinositol-anchored prion protein and Thy-1 differ in lipid composition. *J. Biol. Chem.* **279**, 7530-7536.

Chen, X., Jen, A., Warley, A., Lawrence, M. J., Quinn, P. J. and Morris, R. J. (2009). Isolation at physiological temperature of detergent-resistant membranes with properties expected of lipid rafts: the influence of buffer composition. *Biochem. J.* **417**, 525-533.

Chiu, I., Davis, D. M. and Strominger, J. L. (1999). Trafficking of spontaneously endocytosed MHC proteins. *Proc. Natl. Acad. Sci. USA* **96**, 13944-13949.

Di Pucchio, T., Chatterjee, B., Smed-Sorensen, A., Clayton, S., Palazzo, A., Montes, M., Xue, Y., Mellman, I., Banchereau, J. and Connolly, J. E. (2008). Direct proteasome-independent cross-presentation of viral antigen by plasmacytoid dendritic cells on major histocompatibility complex class I. *Nat. Immunol.* **9**, 551-557.

Drevot, P., Langlet, C., Guo, X. J., Bernard, A. M., Colard, O., Chauvin, J. P., Lasserre, R. and He, H. T. (2002). TCR signal initiation machinery is pre-assembled and activated in a subset of membrane rafts. *EMBO J.* **21**, 1899-1908.

Duncan, L. M., Piper, S., Dodd, R. B., Saville, M. K., Sanderson, C. M., Luzio, J. P. and Lehner, P. J. (2006). Lysine-63-linked ubiquitination is required for endolysosomal degradation of class I molecules. *EMBO J.* **25**, 1635-1645.

Fra, A. M., Williamson, E., Simons, K. and Parton, R. G. (1995). De novo formation of caveolae in lymphocytes by expression of VIP21-caveolin. *Proc. Natl. Acad. Sci. USA* **92**, 8655-8659.

Fujita, A., Cheng, J., Hirakawa, M., Furukawa, K., Kusunoki, S. and Fujimoto, T. (2007). Gangliosides GM1 and GM3 in the living cell membrane form clusters susceptible to cholesterol depletion and chilling. *Mol. Biol. Cell* **18**, 2112-2122.

Glimcher, L. H., Hamano, T., Asofsky, R., Sachs, D. H., Pierres, M., Samelson, L. E., Sharrow, S. O. and Paul, W. E. (1983). IA mutant functional antigen-presenting cell lines. *J. Immunol.* **130**, 2287-2294.

Goebel, J., Forrest, K., Flynn, D., Rao, R. and Roszman, T. L. (2002). Lipid rafts, major histocompatibility complex molecules, and immune regulation. *Hum. Immunol.* **63**, 813-820.

Gomez-Mouton, C., Abad, J. L., Mira, E., Lacalle, R. A., Gallardo, E., Jimenez-Baranda, S., Illa, I., Bernad, A., Manes, S. and Martinez, A. C. (2001). Segregation of leading-edge and uropod components into specific lipid rafts during T cell polarization. *Proc. Natl. Acad. Sci. USA* **98**, 9642-9647.

Griffin, J. P., Chu, R. and Harding, C. V. (1997). Early endosomes and a late endocytic compartment generate different peptide-class II MHC complexes via distinct processing mechanisms. *J. Immunol.* **158**, 1523-1532.

Gromme, M., Uytdehaag, F. G., Janssen, H., Calafat, J., van Binnendijk, R. S., Kenter, M. J., Tulp, A., Verwoerd, D. and Neefjes, J. (1999). Recycling MHC class I molecules and endosomal peptide loading. *Proc. Natl. Acad. Sci. USA* **96**, 10326-10331.

Hancock, J. F. (2006). Lipid rafts: contentious only from simplistic standpoints. *Nat. Rev. Mol. Cell. Biol.* **7**, 456-462.

Harder, T., Scheiffele, P., Verkade, P. and Simons, K. (1998). Lipid domain structure of the plasma membrane revealed by patching of membrane components. *J. Cell Biol.* **141**, 929-942.

Haughton, G., Arnold, L. W., Bishop, G. A. and Mercolino, T. J. (1986). The CH series of murine B cell lymphomas: neoplastic analogues of Ly-1+ normal B cells. *Immunol. Rev.* **93**, 35-51.

Heerklotz, H. (2002). Triton promotes domain formation in lipid raft mixtures. *Biophys. J.* **83**, 2693-2701.

Hiltbold, E. M., Poloso, N. J. and Roche, P. A. (2003). MHC class II-peptide complexes and APC Lipid rafts accumulate at the immunological synapse. *J. Immunol.* **170**, 1329-1338.

Holowka, D., Sheets, E. D. and Baird, B. (2000). Interactions between Fc(epsilon)RI and lipid raft components are regulated by the actin cytoskeleton. *J. Cell Sci.* **113**, 1009-1019.

Huby, R. D., Dearman, R. J. and Kimber, I. (1999). Intracellular phosphotyrosine induction by major histocompatibility complex class II requires co-aggregation with membrane rafts. *J. Biol. Chem.* **274**, 22591-22596.

Jacobson, K., Mouritsen, O. G. and Anderson, R. G. (2007). Lipid rafts: at a crossroad between cell biology and physics. *Nat. Cell Biol.* **9**, 7-14.

Jenei, A., Varga, S., Bene, L., Matyus, L., Bodnar, A., Bacso, Z., Pieri, C., Gaspar, R., Jr, Farkas, T. and Damjanovich, S. (1997). HLA class I and II antigens are partially co-clustered in the plasma membrane of human lymphoblastoid cells. *Proc. Natl. Acad. Sci. USA* **94**, 7269-7274.

Jensen, P. E. (2007). Recent advances in antigen processing and presentation. *Nat. Immunol.* **8**, 1041-1048.

Karacsonyi, C., Knorr, R., Fülbier, A. and Lindner, R. (2004). Association of major histocompatibility complex II with cholesterol- and sphingolipid-rich membranes precedes peptide loading. *J. Biol. Chem.* **279**, 34818-34826.

Karacsonyi, C., Bedke, T., Hinrichsen, N., Schwinzer, R. and Lindner, R. (2005). MHC II molecules and invariant chain reside in membranes distinct from conventional lipid rafts. *J. Leukoc. Biol.* **78**, 1097-1105.

Kirkham, M., Fujita, A., Chadda, R., Nixon, S. J., Kurzchalia, T. V., Sharma, D. K., Pagano, R. E., Hancock, J. F., Mayor, S. and Parton, R. G. (2005). Ultrastructural identification of uncoated caveolin-independent early endocytic vehicles. *J. Cell Biol.* **168**, 465-476.

Kleijmeer, M. J., Escola, J. M., UytdeHaag, F. G., Jakobson, E., Griffith, J. M., Osterhaus, A. D., Stoorvogel, W., Melief, C. J., Rabouille, C. and Geuze, H. J. (2001). Antigen loading of MHC class I molecules in the endocytic tract. *Traffic* **2**, 124-137.

Koch, S., Koch, N., Robinson, P. and Hammerling, G. (1983). Comparison of allogeneic and xenogeneic determinants on the H-2Kk molecule. *Transplantation* **36**, 177-180.

Kumari, S. and Mayor, S. (2008). ARF1 is directly involved in dynamin-independent endocytosis. *Nat. Cell Biol.* **10**, 30-41.

Kusumi, A., Koyama-Honda, I. and Suzuki, K. (2004). Molecular dynamics and interactions for creation of stimulation-induced stabilized rafts from small unstable steady-state rafts. *Traffic* **5**, 213-230.

Lebedeva, T., Anikeeva, N., Kalams, S. A., Walker, B. D., Gaidarov, I., Keen, J. H. and Sykulev, Y. (2004). Major histocompatibility complex class I-intercellular adhesion molecule-1 association on the surface of target cells: implications for antigen presentation to cytotoxic T lymphocytes. *Immunology* **113**, 460-471.

Lichtenberg, D., Goni, F. M. and Heerklotz, H. (2005). Detergent-resistant membranes should not be identified with membrane rafts. *Trends Biochem. Sci.* **30**, 430-436.

Lindner, R. (2001). One-step separation of endocytic organelles, Golgi/trans-Golgi network and plasma membrane by density gradient electrophoresis. *Electrophoresis* **22**, 386-993.

Lindner, R. (2002). Transient surface delivery of invariant chain-MHC II complexes via endosomes: a quantitative study. *Traffic* **3**, 133-146.

Lindner, R. and Unanue, E. R. (1996). Distinct antigen-MHC class II complexes generated by separate processing pathways. *EMBO J.* **15**, 6910-6920.

Liu, T., Zhou, X., Orvell, C., Lederer, E., Ljunggren, H. G. and Jondal, M. (1995). Heat-inactivated Sendai virus can enter multiple MHC class I processing pathways and generate cytotoxic T lymphocyte responses *in vivo*. *J. Immunol.* **154**, 3147-3155.

Lizee, G., Basha, G., Tiong, J., Julien, J. P., Tian, M., Biron, K. E. and Jefferies, W. A. (2003). Control of dendritic cell cross-presentation by the major histocompatibility complex class I cytoplasmic domain. *Nat. Immunol.* **4**, 1065-1073.

Lundmark, R., Doherty, G. J., Howes, M. T., Cortese, K., Vallis, Y., Parton, R. G. and McMahon, H. T. (2008). The GTPase-activating protein GRAF1 regulates the CLIC/GEEC endocytic pathway. *Curr. Biol.* **18**, 1802-1808.

Machy, P., Truneh, A., Gennaro, D. and Hoffstein, S. (1987). Major histocompatibility complex class I molecules internalized via coated pits in T lymphocytes. *Nature* **328**, 724-726.

Madore, N., Smith, K. L., Graham, C. H., Jen, A., Brady, K., Hall, S. and Morris, R. (1999). Functionally different GPI proteins are organized in different domains on the neuronal surface. *EMBO J.* **18**, 6917-6926.

Matko, J., Bushkin, Y., Wei, T. and Edidin, M. (1994). Clustering of class I HLA molecules on the surfaces of activated and transformed human cells. *J. Immunol.* **152**, 3353-3360.

Matsuki, Y., Ohmura-Hoshino, M., Goto, E., Aoki, M., Mito-Yoshida, M., Uematsu, M., Hasegawa, T., Koseki, H., Ohara, O., Nakayama, M. et al. (2007). Novel regulation of MHC class II function in B cells. *EMBO J.* **26**, 846-854.

Mayor, S. and Pagano, R. E. (2007). Pathways of clathrin-independent endocytosis. *Nat. Rev. Mol. Cell. Biol.* **8**, 603-612.

Meyer zum Bueschenfelde, C. O., Unternaehrer, J., Mellman, I. and Bottomly, K. (2004). Regulated recruitment of MHC class II and costimulatory molecules to lipid rafts in dendritic cells. *J. Immunol.* **173**, 6119-6124.

Morrissey, J. H. (1981). Silver stain for proteins in polyacrylamide gels: a modified procedure with enhanced uniform sensitivity. *Anal. Biochem.* **117**, 307-310.

Munro, S. (2003). Lipid rafts: elusive or illusive? *Cell* **115**, 377-388.

Naslavsky, N., Weigert, R. and Donaldson, J. G. (2003). Convergence of non-clathrin- and clathrin-derived endosomes involves Arf6 inactivation and changes in phosphoinositides. *Mol. Biol. Cell* **14**, 417-431.

Naslavsky, N., Weigert, R. and Donaldson, J. G. (2004). Characterization of a nonclathrin endocytic pathway: membrane cargo and lipid requirements. *Mol. Biol. Cell* **15**, 3542-3552.

Orlandi, P. A. and Fishman, P. H. (1998). Filipin-dependent inhibition of cholera toxin: evidence for toxin internalization and activation through caveolae-like domains. *J. Cell Biol.* **141**, 905-915.

Pathak, S. S. and Blum, J. S. (2000). Endocytic recycling is required for the presentation of an exogenous peptide via MHC class II molecules. *Traffic* **1**, 561-569.

Pike, L. J. (2004). Lipid rafts: heterogeneity on the high seas. *Biochem. J.* **378**, 281-292.

Pike, L. J. (2006). Rafts defined: a report on the keystone symposium on lipid rafts and cell function. *J. Lipid Res.* **47**, 1597-1598.

Pinet, V., Malnati, M. S. and Long, E. O. (1994). Two processing pathways for the MHC class II-restricted presentation of exogenous influenza virus antigen. *J. Immunol.* **152**, 4852-4860.

Pinet, V., Vergelli, M., Martin, R., Bakke, O. and Long, E. O. (1995). Antigen presentation mediated by recycling of surface HLA-DR molecules. *Nature* **375**, 603-606.

Prior, I. A., Muncke, C., Parton, R. G. and Hancock, J. F. (2003). Direct visualization of Ras proteins in spatially distinct cell surface microdomains. *J. Cell Biol.* **160**, 165-170.

Rock, K. L. and Shen, L. (2005). Cross-presentation: underlying mechanisms and role in immune surveillance. *Immunol. Rev.* **207**, 166-183.

Rodgers, W. and Smith, K. (2005). Properties of glycolipid-enriched membrane rafts in antigen presentation. *Crit. Rev. Immunol.* **25**, 19-30.

Röper, K., Corbeil, D. and Huttner, W. B. (2000). Retention of prominin in microvilli reveals distinct cholesterol-based lipid micro-domains in the apical plasma membrane. *Nat. Cell Biol.* **2**, 582-592.

Sabharanjak, S., Sharma, P., Parton, R. G. and Mayor, S. (2002). GPI-anchored proteins are delivered to recycling endosomes via a distinct cdc42-regulated, clathrin-independent pinocytic pathway. *Dev. Cell* **2**, 411-423.

Schirmbeck, R., Bohm, W., Melber, K. and Reimann, J. (1995). Processing of exogenous heat-aggregated (denatured) and particulate (native) hepatitis B surface antigen for class I-restricted epitope presentation. *J. Immunol.* **155**, 4676-4684.

Schuck, S., Honsho, M., Ekroos, K., Shevchenko, A. and Simons, K. (2003). Resistance of cell membranes to different detergents. *Proc. Natl. Acad. Sci. USA* **100**, 5795-5800.

Setterblad, N., Roucard, C., Bocaccio, C., Abastado, J. P., Charron, D. and Mooney, N. (2003). Composition of MHC class II-enriched lipid microdomains is modified during maturation of primary dendritic cells. *J. Leukoc. Biol.* **74**, 40-48.

Setterblad, N., Becart, S., Charron, D. and Mooney, N. (2004). B cell lipid rafts regulate both peptide-dependent and peptide-independent APC-T cell interaction. *J. Immunol.* **173**, 1876-1786.

Sharma, P., Varma, R., Sarasij, R. C., Ira Gousset, K., Krishnamoorthy, G., Rao, M. and Mayor, S. (2004). Nanoscale organization of multiple GPI-anchored proteins in living cell membranes. *Cell* **116**, 577-589.

Shin, J. S., Ebersold, M., Pypaert, M., Delamarre, L., Hartley, A. and Mellman, I. (2006). Surface expression of MHC class II in dendritic cells is controlled by regulated ubiquitination. *Nature* **444**, 115-118.

Sinnathamby, G. and Eisenlohr, L. C. (2003). Presentation by recycling MHC class II molecules of an influenza hemagglutinin-derived epitope that is revealed in the early endosome by acidification. *J. Immunol.* **170**, 3504-3513.

Sloma, I., Zilber, M. T., Vasselon, T., Setterblad, N., Cavallari, M., Mori, L., De Libero, G., Charron, D., Mooney, N. and Gelin, C. (2008). Regulation of CD1a surface expression and antigen presentation by invariant chain and lipid rafts. *J. Immunol.* **180**, 980-987.

Szollosi, J., Horejsi, V., Bene, L., Angelisova, P. and Damjanovich, S. (1996). Supramolecular complexes of MHC class I, MHC class II, CD20, and tetraspan molecules (CD53, CD81, and CD82) at the surface of a B cell line JY. *J. Immunol.* **157**, 2939-2946.

Tiwari, N., Garbi, N., Reinheckel, T., Moldenhauer, G., Hammerling, G. J. and Momburg, F. (2007). A transporter associated with antigen-processing independent vacuolar pathway for the MHC class I-mediated presentation of endogenous transmembrane proteins. *J. Immunol.* **178**, 7932-7942.

Torgersen, M. L., Skretting, G., van Deurs, B. and Sandvig, K. (2001). Internalization of cholera toxin by different endocytic mechanisms. *J. Cell Sci.* **114**, 3737-3747.

Umemura, Y. M., Vrljic, M., Nishimura, S. Y., Fujiwara, T. K., Suzuki, K. G. and Kusumi, A. (2008). Both MHC class II and its GPI-anchored form undergo hop diffusion as observed by single-molecule tracking. *Biophys. J.* **95**, 435-450.

Valentine, R. C., Shapiro, B. M. and Stadtman, E. R. (1968). Regulation of glutamine synthetase. XII. Electron microscopy of the enzyme from Escherichia coli. *Biochemistry* **7**, 2143-2152.

Vamosi, G., Bodnar, A., Vereb, G., Jenei, A., Goldman, C. K., Langowski, J., Toth, K., Matyus, L., Szollosi, J., Waldmann, T. A. et al. (2004). IL-2 and IL-15 receptor alpha-subunits are coexpressed in a supramolecular receptor cluster in lipid rafts of T cells. *Proc. Natl. Acad. Sci. USA* **101**, 11082-11087.

van Niel, G., Wubbolts, R., Ten Broeke, T., Buschow, S. I., Ossendorp, F. A., Melief, C. J., Raposo, G., van Balkom, B. W. and Stoorvogel, W. (2006). Dendritic cells regulate exposure of MHC class II at their plasma membrane by oligoubiquitination. *Immunity* **25**, 885-894.

van Rheenen, J., Achame, E. M., Janssen, H., Calafat, J. and Jalink, K. (2005). PIP2 signaling in lipid domains: a critical re-evaluation. *EMBO J.* **24**, 1664-1673.

Vega, M. A. and Strominger, J. L. (1989). Constitutive endocytosis of HLA class I antigens requires a specific portion of the intracytoplasmic tail that shares structural features with other endocytosed molecules. *Proc. Natl. Acad. Sci. USA* **86**, 2688-2692.

Vrljic, M., Nishimura, S. Y., Brasselet, S., Moerner, W. E. and McConnell, H. M. (2002). Translational diffusion of individual class II MHC membrane proteins in cells. *Biophys. J.* **83**, 2681-1692.

Walseng, E., Bakke, O. and Roche, P. A. (2008). MHC class II-peptide complexes internalize using a clathrin- and dynamin-independent endocytosis pathway. *J. Biol. Chem.* **283**, 14717-14727.

Watts, C. (2004). The exogenous pathway for antigen presentation on major histocompatibility complex class II and CD1 molecules. *Nat. Immunol.* **5**, 685-692.

Wilson, B. S., Steinberg, S. L., Liederman, K., Pfeiffer, J. R., Surviladze, Z., Zhang, J., Samelson, L. E., Yang, L. H., Kotula, P. G. and Oliver, J. M. (2004). Markers for detergent-resistant lipid rafts occupy distinct and dynamic domains in native membranes. *Mol. Biol. Cell* **15**, 2580-2592.

Zhong, G., Romagnoli, P. and Germain, R. N. (1997). Related leucin-based cytoplasmic targeting signals in invariant chain and major histocompatibility complex class II molecules control endocytic presentation of distinct determinants in a single protein. *J. Exp. Med.* **185**, 429-438.